ARTICLES

Journal of Semiconductors
(2019) 40, 032101
doi: 10.1088/1674-4926/40/3/032101

Growth behavior and electronic properties of Ge_{n+1} and $AsGe_n$ (n = 1–20) clusters: a DFT study

M. Benaida[1, †], K. E. Aiadi[1], S. Mahtout[2], S. Djaadi[1], W. Rammal[3], and M. Harb[4, †]

[1]Laboratoire de Développement des Energies Nouvelles et Renouvelables en Zones Aride, Université de Ouargla, 30000 Ouargla, Algeria

[2]Laboratoire de Physique Théorique, Faculté des Sciences Exactes, Université de Bejaia, 06000 Begaia, Algeria

[3]Faculty of Sciences, Lebanese University, Lebanon

[4]KAUST Catalysis Center (KCC), Physical Sciences and Engineering Division (PSE), King Abdullah University of Science and Technology (KAUST), Thuwal 23955-6900, Saudi Arabia

Abstract: We present a systematic computational study based on the density functional theory (DFT) aiming to high light the possible effects of one As doping atom on the structural, energetic, and electronic properties of different isomers of Ge_{n+1} clusters with n = 1–20 atoms. By considering a large number of structures for each cluster size, the lowest-energy isomers are determined. The lowest-energy isomers reveal three-dimensional structures starting from n = 5. Their relative stability versus atomic size is examined based on the calculated binding energy, fragmentation energy, and second-order difference of energy. Doping Ge_{n+1} clusters with one As atom does not improve their stability. The electronic properties as a function of the atomic size are also discussed from the calculated HOMO–LUMO energy gap, vertical ionization potential, vertical electron affinity, and chemical hardness. The obtained results are significantly affected by the inclusion of one As atom into a Ge_n cluster.

Key words: density functional theory; As–Ge clusters; structural properties; electronic properties

Citation: M Benaida, K E Aiadi, S Mahtout, S Djaadi, W Rammal, and M Harb, Growth behavior and electronic properties of Ge_{n+1} and $AsGe_n$ (n = 1 –20) clusters: a DFT study[J]. *J. Semicond.*, 2019, 40(3), 032101. http://doi.org/10.1088/1674-4926/40/3/032101

1. Introduction

Studying clusters of various chemical elements has become a modern research topic in both physical and chemical communities over the last four decades[1, 2], due to the size-dependent evolution of their fundamental properties and their technological applications in large variety of research fields, from catalysis to optoelectronics. Their particular structural, energetic, and electronic properties are fully understood and still constitute the subject of many research projects[3, 4]. Nanoscale materials (called clusters) with various sizes can provide different behaviors to that of the bulk material. The physical and chemical features of bimetallic clusters are dependent not only on the size and shape but also on the chemical composition and the atomic arrangement of the two metal elements[2]. Therefore, studying the changes in the structural and electronic properties of the cluster with its size has become important[4, 5]. Several theoretical calculations have been performed on pure and mixed neutral and charged clusters of group 14 elements[6, 7] especially silicon and germanium.

Numerous theoretical and experimental studies on Ge clusters have been published over the last decade[8] and different types of structures have been proposed[9, 10]. Theoretically, several computations have concluded that Ge_n cages can be stabilized through the encapsulation of guest atom inside the cage. This was seen before in Si_n cages. Matthias Brack *et al.*[11] presented the global minimum of $CuGe_{10}^+$ clusters as a magic number along with D_{4d} symmetry. Han *et al.*[12] have presented a theoretical investigation of very small Ge_n (n = 1–4) clusters doped by Sn, and they found a charge transfer from Sn to Ge atoms. Singh *et al.*[13] have reported that the n capsulation can be utilized for stabilizing highly symmetric Ge_n cages having from 16 to 20 atoms. Wang and Han[14] have investigated $CuGe_n$ (n = 2–13) clusters and shown that Cu doping can decreaseits binding energies, and so, the stability of Ge_{n+1} clusters. Zhao and Wang have studied in 2009 Mn-doped Ge_n clusters[15] and shown that Mn dopant can contribute to the stability increase of Ge_{n+1} clusters. Jaiswal and Kumarusing studied the atomic and electronic structures of both neutral and negatively charged $ZrGe_n$ (n = 1–21) clusters using ab-initio calculations[16] and predicted cage-like stable geometries for $n \geqslant 13$. Siouani *et al.*[10] have investigated systematically the equilibrium geometries and electronic properties of VGe_n (n = 1–19) clusters and found that V atom in VGe_n can make the stability stronger starting from n = 7. More recently, Mahtout *et al.*[17] have studied the structural, energetic, and electronic properties of MGe_n clusters with M = Cu, Ag, Au and n = 1–19 using DFT approach. They have found the endohedral structures where the metal atom was incorporated inside the Ge_{n+1} cage appear at n = 10 when the dopant is Cu and at n = 12 for Ag or Au. Djaadi *et al.*[18] have investigated the structures and relative stability of pure Ge_{n+1}, neutral cationic and anionic $SnGe_n$ (n = 1–17) clusters. They found that the Sn atom occupied a peripheral position for $SnGe_n$ clusters when $n < 12$ and occupied a core position for $n > 12$.

Here, we report a systematic computational study based on the density functional theory (DFT) aiming to highlight the possible effects of one arsenic atom on the structural, energet-

Correspondence to: M Benaida, meriembenaida@gmail.com; M Harb, moussab.harb@kaust.edu.sa

Received 4 AUGUST 2018; Revised 27 SEPTEMBER 2018.

Table 1. Averaged bond length *a*, binding energy E_b, vertical ionization potential VIP, and vertical electron affinity VEA for Ge_2, Ge_3 and As_2.

Symmetry	Our work				Bibliographic date[24-40]			
	a (Å)	E_b (eV)	VIP (eV)	VEA (eV)	*a* (Å)	E_b (eV)	VIP (eV)	VEA (eV)
Ge_2	2.503	1.445	7.362	1.473	2.450	1.446	7.844	1.900
					2.413	~1.430	7.627	1.751
					2.540	1.620	7.934	1.549
					2.610	1.812		
					2.570	~1.350		
					2.420	1.410		
					2.440	1.320		
					2.421	1.230		
					2.625	1.280		
Ge_3	2.370	2.110	8.024	1.306	2.546	2.059	7.804	2.200
					2.400	2.240		
					2.476	2.150		
						2.040		
						1.860		
As_2	2.143	1.686	9.677	0.132	2.189	1.763		
					2.103			
					2.192			

ic, and electronic properties of different isomers of Ge_{n+1} in the atomic size range n = 1–20 atoms. We believe this work is useful for deeply understanding the effects of incorporating one As atom into Ge_{n+1} clusters and can be considered as a guideline for future experiments. To the best of our knowledge, no systematic study has been addressed on neutral and charged $AsGe_n$ clusters.

2. Computational methods

The electronic structure calculations of $AsGe_n^q$ (n = 1–20, q = 0, ± 1) clusters were performed using the density functional theory (DFT)[19] as implemented in the SIESTA program[20]. This code uses norm-conserving Troullier-Martins nonlocal pseudopotentials[2, 21] and employs flexible basis sets of localized Gaussian-type atomic orbitals[2]. The exchange correlation energy was evaluated using the generalized gradient approximation (GGA) parameterized by Perdew and Zunger[22] and by Perdew, Burke, and Ernserh of (PBE)[23]. The self-consistent field (SCF) calculations were carried out with convergence criterion of 1×10^{-4} a.u. for total energy. We used a double ζ (DZ) basis with polarization function for As and Ge atoms. With energy shift parameter of 50 meV, the change density was calculated in regular real-space grid with cut-off energy of 150 Ry. The simulated clusters were placed in a big cubic supercell with a parameter of 40 Å, including enough vacuums between neighboring clusters and periodic boundary conditions were imposed. To sample the Brillouin zone, only a single *k*-point centered at Γ was used because of the extended size of the supercell. The conjugated gradient method within Hellmann-Feynman forces was used and all the forces after structural relaxation were less than 10^{-3} eV/Å.

We first searched for the lowest-energy structures of pure Ge_{n+1} clusters in the 1–20 atoms range by exploring various possibilities of isomers. Secondly, the most stable ground state structures obtained for Ge_{n+1} clusters were doped through substitution with one As atom. Then, the obtained $AsGe_n$ clusters were optimized until reaching their ground states. In order to get lowest-energy structures of the $AsGe_n$ clusters, several initials isomeric structures, including some high and low symmetries, were optimized by placing one As atom in substitution in different possible sites of the pure corresponding Ge_{n+1} in order to get as close as possible to the low energy structures. Then, we cannot be sure that a more stable structure than those found in our calculations does not exist. We aim of our study is to highlight the variation of the properties of germanium cage clusters due to the As doping atom. We hope that this work would be useful to understand the influence of the As atom on the properties of germanium clusters and provide some guidelines for the probable future experimental studies. To check the validity of our computational method, benchmark tests have been done on Ge_2, Ge_3, and As_2 parameters. The values are reported in Table 1 together with available theoretical and experimental results. Our calculated results were found to be in line with the literature, confirming the reliability of our protocol to simulate small Ge clusters.

3. Results and discussion

3.1. Structural analysis

We report in Fig. 1 the lowest-energy structures obtained for Ge_{n+1} (n = 1–20) and their corresponding isomers. Their energetic ordering is reported in Table 2. Our calculations reveal that almost all atoms are on the surface. Until n = 20, prolate-type geometries are in competition with the nearly spherical ones. The calculated results for the most favorable isomers are given in bold character. The most stable structures for n + 1 = 2, 3, and 4 adopt a planar disposition in line with previous works[10, 14, 18, 24, 25] using DFT different calculations. The triangular geometry with C_{2v} symmetry is found to be the lowest-energy structure for Ge_3. The lowest-energy isomer of the tetramer Ge_4 has D_{2h} symmetry in line with previous findings[15, 18, 20, 26, 27]. The most favorable isomer for Ge_5 cluster reveals a triangular bipyramid disposition with D_{3h} symmetry, which is also in line with the previous data[10, 14, 24, 26]. The lowest-energy Ge_6 cluster has bicapped quadrilateral structure with C_{2v} symmetry, in good agreement with the previous data[10, 18, 26]. For Ge_7 cluster, the most stable structure reveals

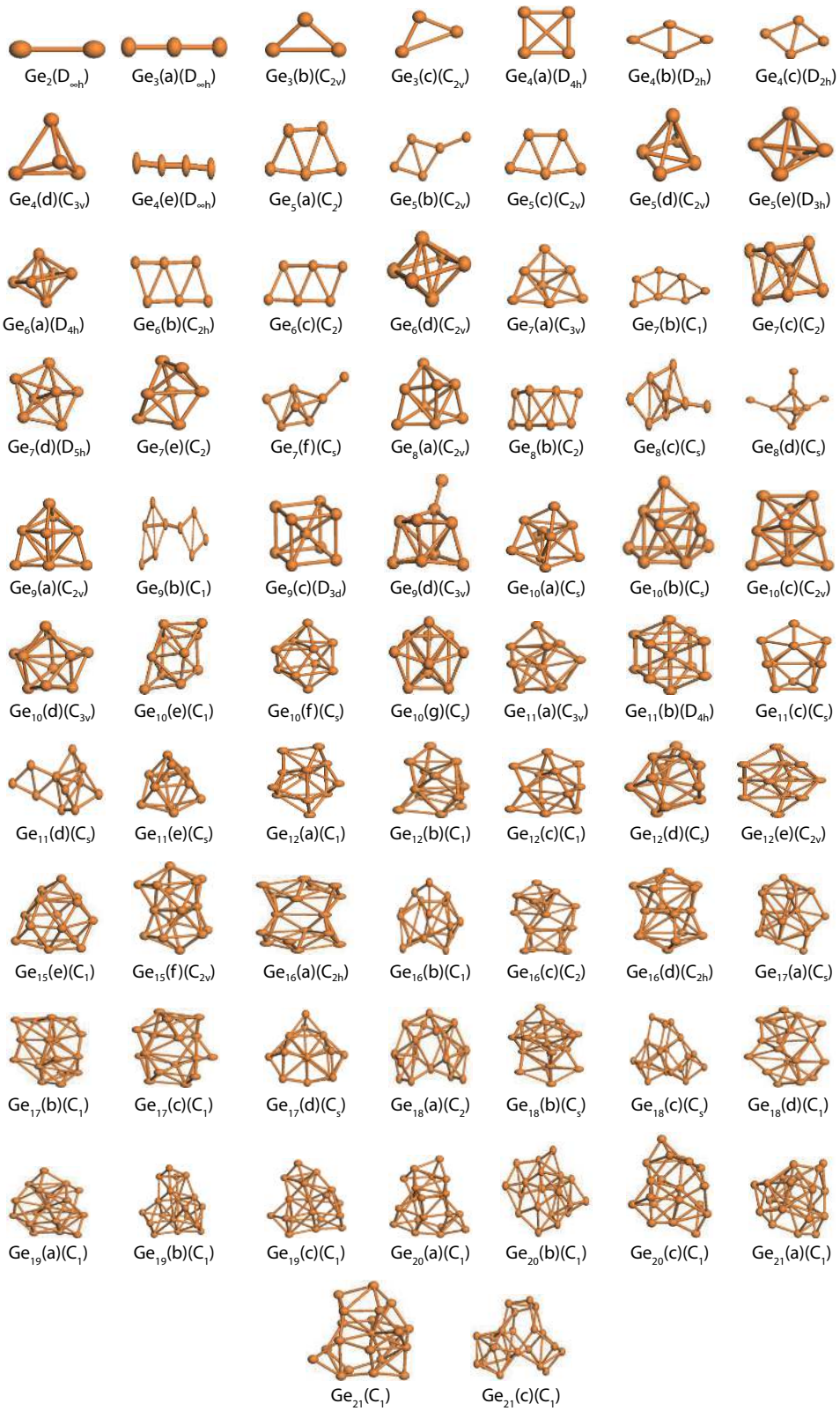

Fig. 1. (Color online) Most favorable structures together with their corresponding isomers for Ge_{n+1} (n = 1–20) clusters.

a pentagonal bipyramid of D_{5h} symmetry. Other researchers also previously obtained similar results for Ge_7[10, 14, 24, 26]. For Ge_8 clusters, the most stable isomer shows a capped pentagonal bipyramid disposition of C_{2v} symmetry, as obtained in earlier works[20, 28]. Ge_9 is a capped pentagonal bipyramid structure of C_{2v} symmetry. The most favorable isomer of Ge_{10} cluster is a capped pentagonal basis structure and has C_{3v} symmetry. The lowest-energy Ge_{11} cluster shows a compact near spherical geometry of C_s symmetry. As per Ge_{12} and Ge_{13} clusters, prolate-type structure with C_{2v} symmetry was always preferred. The shape of Ge_{14} is a prolate structure with C_s symmetry. For Ge_{15} and Ge_{16} clusters, prolate-type geometry was obtained with C_{2v} and C_{2h} symmetries, respectively. The lowest-energy isomer for Ge_{17} possesses a near spherical geo-

Table 2. Group of symmetry, E_b, ΔE, VIP, VEA, η, and a_{Ge-Ge} for pure Ge_{n+1} (n = 1 – 20) clusters.

Cluster size (n)	Symmetry	E_b (eV/atom)	ΔE (eV)	VEA (eV)	VIP (eV)	η (eV)	a_{Ge-Ge} (Å)
1	$D_{\infty h}$	1.445	0.265	7.362	1.473	5.889	2.503
2	$D_{\infty h}$	2.048	1.272	7.557	1.476	6.081	2.339
	C_{2v}	2.109	1.543	8.024	1.305	6.719	2.370
	C_{2v}	2.110	1.543	8.024	1.306	6.718	2.370
3	D_{4h}	2.228	0.455	6.834	1.599	5.235	2.550
	D_{2h}	2.556	1.180	7.734	1.758	5.976	2.576
	D_{2h}	2.557	1.179	7.733	1.758	5.976	2.597
	C_{3v}	2.078	0.660	7.056	1.717	5.339	2.479
	$D_{\infty h}$	2.061	1.169	7.114	2.102	5.012	2.346
4	C_2	2.518	1.089	6.911	2.149	4.762	2.606
	C_{2v}	2.450	1.026	6.766	2.207	4.559	2.564
	C_{2v}	2.499	0.808	6.774	2.070	4.704	2.618
	C_{2v}	2.504	0.577	7.588	2.560	5.028	2.775
	D_{3h}	2.707	2.036	8.672	0.218	8.454	2.547
5	D_{4h}	2.847	1.998	7.777	1.372	6.405	2.782
	C_{2h}	2.668	1.236	7.142	1.820	5.322	2.760
	C_2	2.672	1.386	7.172	1.790	5.382	2.606
	C_{2v}	2.848	1.957	7.742	1.359	6.383	2.710
6	D_{3v}	2.877	2.350	7.460	1.064	6.396	2.734
	C_1	2.687	0.164	7.304	1.673	5.631	2.647
	C_2	2.843	1.170	7.034	1.749	5.285	2.754
	D_{5h}	2.974	1.836	7.875	1.774	6.101	2.747
	C_2	2.843	1.170	7.034	1.748	5.286	2.754
	C_s	2.617	0.755	6.620	2.102	4.518	2.701
7	C_{2v}	2.866	0.980	7.216	2.232	4.984	2.776
	C_2	2.735	0.977	6.937	2.194	4.743	2.658
	C_s	2.739	0.708	6.556	2.212	4.344	2.730
	C_s	2.422	0.431	6.194	2.805	3.389	2.651
8	C_{2v}	2.985	1.654	7.126	1.570	5.556	2.782
	C_1	2.700	1.066	6.849	2.394	4.455	2.570
	D_{3d}	2.574	0.227	6.288	2.271	4.017	2.798
	C_{3v}	2.827	1.102	7.068	2.313	4.755	2.686
9	C_s	2.848	1.459	6.462	2.146	4.316	2.742
	C_s	3.002	1.753	7.137	1.662	5.475	2.779
	C_{2v}	2.968	1.379	7.070	1.981	5.089	2.785
	C_{3v}	3.082	1.812	7.432	1.857	5.575	2.775
	C_1	2.953	1.295	6.900	1.913	4.987	2.738
	C_s	3.013	1.015	7.152	2.393	4.759	2.794
	C_s	3.003	1.547	7.410	1.383	6.027	2.771
10	C_{3v}	2.792	1.063	6.402	2.364	4.038	2.714
	D_{4h}	2.715	0.793	6.326	1.975	4.351	2.816
	C_s	2.907	0.962	6.605	2.084	4.521	2.748
	C_s	2.892	0.990	6.820	2.318	4.502	2.724
	C_s	3.029	1.258	7.107	1.332	5.775	2.770
11	C_s	2.936	0.803	6.852	2.547	4.305	2.798
	C_1	2.955	0.916	6.759	2.345	4.414	2.784
	C_1	2.964	1.059	6.696	2.175	4.521	2.801
	C_s	2.979	0.370	6.656	2.780	3.876	2.793
	C_{2v}	3.032	1.793	7.402	1.258	6.144	2.744
12	C_{2v}	3.050	1.181	8.243	1.290	6.953	2.760
	C_2	3.007	1.153	1.153	2.390	4.553	2.792
	C_1	3.015	0.945	6.785	2.412	4.373	2.835
	C_s	2.990	1.130	6.608	2.102	4.506	2.769
	C_1	3.015	0.944	7.302	1.779	5.523	2.831
13	C_{3v}	2.922	0.987	5.967	2.633	3.334	2.696
	C_s	3.026	1.107	6.625	2.179	4.446	2.700
	O_h	2.977	1.007	6.915	3.095	3.820	2.659
	C_1	2.986	1.036	6.471	2.127	4.344	2.784
	C_s	3.092	1.628	7.486	1.539	5.947	2.797
14	D_{3d}	2.864	0.495	6.726	2.977	3.749	2.666
	C_1	2.999	1.234	6.800	2.311	4.489	2.829
	C_s	2.959	0.941	6.553	2.393	4.160	2.785
	C_1	3.022	1.149	6.579	2.178	4.401	2.812
	C_1	3.023	1.156	6.927	2.468	4.459	2.786
	C_{2v}	3.082	0.899	7.339	1.851	5.488	2.814

Continued from Table 2

Cluster size (n)	Symmetry	E_b (eV/atom)	ΔE (eV)	VEA (eV)	VIP (eV)	η (eV)	a_{Ge-Ge} (Å)
15	C_{2h}	3.027	1.436	6.840	2.308	4.532	2.715
	C_1	3.020	0.883	6.555	2.494	4.061	2.755
	C_2	3.034	1.364	6.755	2.262	4.493	2.808
	C_{2h}	3.095	1.393	7.548	1.753	5.795	2.780
16	C_s	3.050	1.103	6.588	2.343	4.245	2.781
	C_1	3.043	1.254	6.696	2.428	4.268	2.772
	C_1	3.038	1.022	6.616	2.500	4.116	2.762
	C_s	3.077	0.858	7.075	1.716	5.359	2.823
17	C_2	3.014	0.864	6.493	2.590	3.903	2.869
	C_s	3.013	0.948	6.537	2.537	4.000	2.790
	C_s	3.009	0.555	6.400	2.815	3.585	2.782
	C	3.062	1.452	7.152	1.486	5.666	2.729
18	C_1	3.053	0.966	6.473	2.477	3.996	2.843
	C_1	3.019	0.779	6.516	2.728	3.788	2.771
	C_1	3.019	0.780	6.517	2.727	3.790	2.771
19	C_1	3.046	0.828	6.387	2.596	3.791	2.735
	C_1	3.033	0.962	6.365	2.455	3.910	2.768
	C_1	3.001	0.828	6.418	2.650	3.768	2.781
20	C_1	3.041	0.743	6.372	2.679	3.693	2.769
	C_1	3.061	3.061	6.403	2.845	3.558	2.735
	C_1	3.050	0.559	6.182	2.734	3.448	2.761

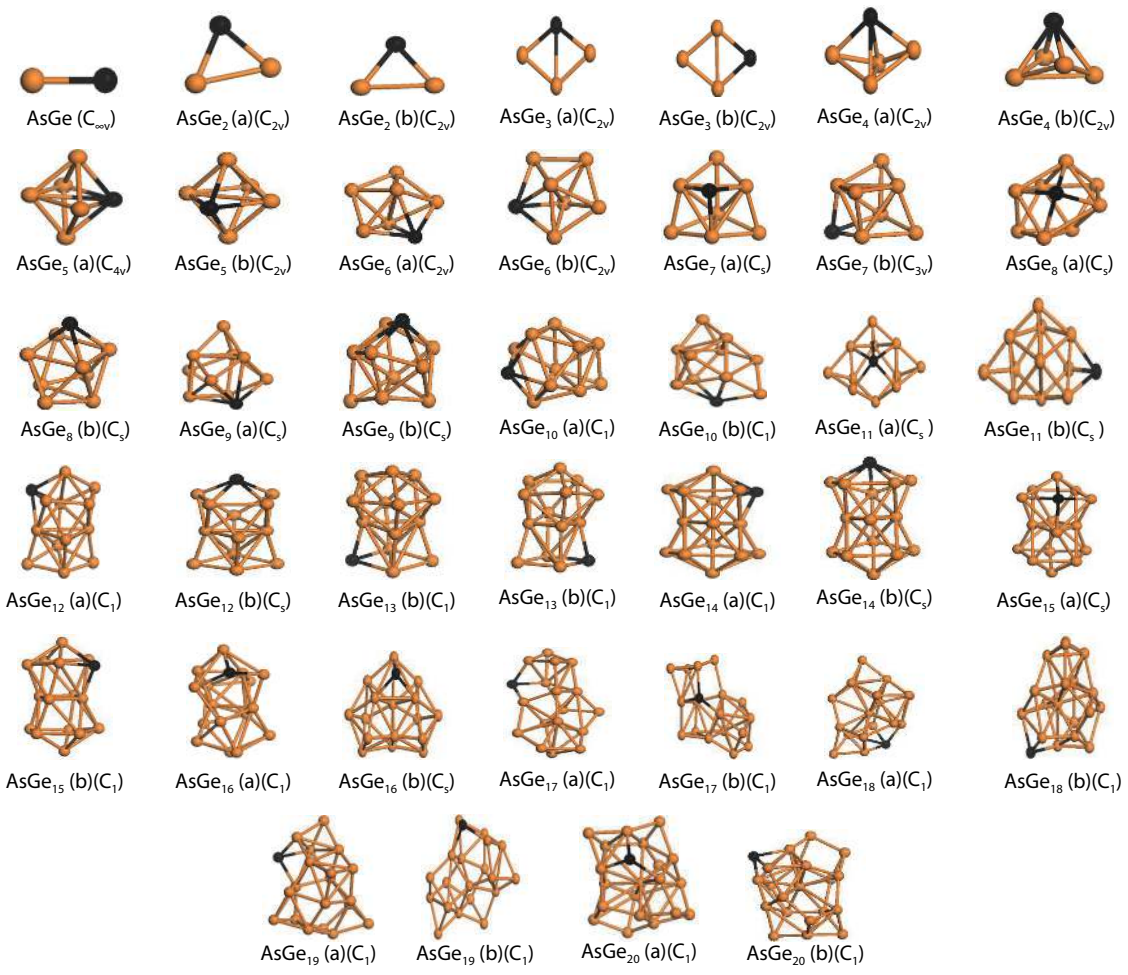

Fig. 2. (Color online) Most favorable structures and their corresponding isomers of $AsGe_n$ (n = 1–20) clusters.

metry of C_s symmetry. From Ge_{18} to Ge_{21} clusters, prolate-type shape with C_1 symmetry was always preferred.

The most favorable geometries of $AsGe_n$ (n = 1–20) clusters and their corresponding isomers are summarized in Fig. 2, whereas their energetic ordering is reported in Table 3. The $AsGe_n$ clusters adopt somehow similar structures to their corresponding Ge_{n+1} except for n = 8, 10, 11, and 16. In all cases, the arsenic atom is always located on the surface. The

Table 3. Group of symmetry, E_b, ΔE, VEA, VIP, η, and a_{Ge-Ge}, a_{As-Ge} for $AsGe_n$ (n = 1–20) clusters.

Cluster size (n)	Symmetry	E_b (eV/atom)	ΔE (eV)	VEA (eV)	VIP (eV)	η (eV)	a_{Ge-Ge} (Å)	a_{As-Ge} (Å)
1	(a)$C_{\infty v1}$	1.426	0.171	2.175	8.142	5.967	-	2.350
2	(a)C_{2v}	2.139	1.110	0.969	7.425	6.456	2.775	2.445
	(b)C_{2v}	2.139	1.109	0.778	8.198	7.410	2.775	2.445
3	(a)C_{2v}	2.380	0.589	1.440	6.704	5.264	2.603	2.543
	(b)C_{2v}	2.418	1.266	1.726	7.377	5.651	2.661	2.473
4	(a)C_{2v}	2.575	0.208	0.451	8.640	8.189	2.738	2.661
	(b)C_{2v}	2.641	0.917	0.124	8.809	8.685	2.692	2.734
5	(a)C_{4v}	2.705	1.116	0.928	6.657	5.729	2.807	2.679
	(b)C_{2v}	2.702	1.058	1.088	6.951	5.863	2.782	2.706
6	(a)C_{2v}	2.837	1.279	1.632	6.614	4.982	2.786	2.703
	(b)C_{2v}	2.837	1.278	1.632	6.615	4.983	2.786	2.704
7	(a)C_s	2.814	0.503	2.060	7.179	5.119	2.788	2.635
	(b)C_{3v}	2.835	0.743	1.701	7.022	5.321	2.821	2.567
8	(a)C_s	2.908	0.571	1.279	6.661	5.382	2.808	2.678
	(b)C_s	2.909	0.571	1.279	6.661	5.382	2.808	2.678
9	(a)C_s	2.977	1.066	1.604	6.271	4.667	2.774	2.819
	(b)C_s	2.977	1.064	1.603	6.271	4.668	2.774	2.819
10	(a)C_1	2.949	0.759	1.051	6.663	5.612	2.793	2.697
	(b)C_1	2.949	0.898	0.884	6.953	6.069	2.774	2.716
11	(a)C_s	2.945	1.026	0.783	6.609	5.826	2.740	2.813
	(b)C_s	2.940	0.773	1.305	6.481	5.176	2.775	2.596
12	(a)C_1	2.993	0.393	1.019	8.052	7.033	2.788	2.693
	(b)C_s	3.003	0.396	1.044	7.736	6.692	2.814	2.667
13	(a)C_1	3.016	0.696	1.518	6.578	5.060	2.826	2.606
	(b)C_1	3.016	0.697	1.520	6.574	5.054	2.780	2.607
14	(a)C_1	3.042	0.581	1.248	7.125	5.877	2.821	2.681
	(b)C_s	3.046	0.797	1.174	6.946	5.772	2.828	2.783
15	(a)C_s	3.045	0.782	1.482	6.984	5.502	2.801	2.736
	(b)C_1	3.043	0.846	1.300	6.917	5.617	2.817	2.719
16	(a)C_1	3.045	0.538	1.394	6.977	5.583	2.813	2.595
	(b)C_s	3.035	0.810	1.547	6.823	5.276	2.830	2.593
17	(a)C_1	3.031	0.623	0.763	7.031	6.268	2.766	2.566
	(b)C_1	3.030	0.390	0.453	7.310	6.857	2.747	2.556
18	(a)C_1	3.017	0.627	1.867	6.346	4.479	2.777	2.629
	(b)C_1	3.024	0.594	2.000	6.361	4.361	2.803	2.592
19	(a)C_1	3.023	0.559	1.916	6.098	4.182	2.769	2.581
	(b)C_1	3.029	0.519	1.667	6.834	5.167	2.732	2.580
20	(a)C_1	3.065	0.667	1.961	6.558	4.597	2.739	2.573
	(b)C_1	3.059	0.579	1.870	6.937	5.067	2.745	2.601

$AsGe_2$ cluster shows a triangular geometry of C_{2v} symmetry with two equivalent As–Ge bonds of 2.445 Å and one Ge–Ge bond of 2.775 Å. The As–Ge bond distance of 0.09 Å is larger than that in AsGe dimer. The most stable structure of $AsGe_3$ cluster presents a planar C_{2v} symmetry with a binding energy of 2.418 eV/atom, which is smaller than that of tetramer Ge_4 (2.557 eV/atom). For $AsGe_4$, a distorted rectangular pyramid with C_{2v} symmetry is found with a binding energy of 0.066 eV/atom, which is also smaller thanGe_5. The Ge–Ge and As–Ge bond lengths are 2.692 and 2.734 Å, respectively. For $AsGe_5$, the As atom is located at the convex site of a quasi-rectangular bipyramid structure of C_{4v} symmetry, As–Ge bond distance of 2.679 Å, and an average Ge–Ge bond distance of 2.807 Å. The lowest energy isomer for $AsGe_6$ cluster is a structure with C_{2v} point group symmetry, As–Ge bond length of 2.704 Å, and an average Ge–Ge bond distance of 2.786 Å. For $AsGe_7$ cluster, the lowest-energy isomer reveals a low-lying structure with a planar C_{3v} symmetry and a binding energy of 2.835 eV/atom, which is smaller than that for tetramer Ge_8 (2.866 eV/atom). For $AsGe_8$ cluster, its binding energy of only 0.076 eV/atom is also smaller than that obtained for Ge_9 cluster with C_s symmetry of the ground state isomer. The lowest-energy structure of $AsGe_9$ cluster has C_s symmetry combining two irregular hexagonal prisms with As atom on top of one of them. The ground state geometry of $AsGe_{10}$ has C_1 point group symmetry. The As atom tends to be stabilized on the surface. For n = 11, 12, 13, 14, 15, 16, and 17, prolate structures were found to be the most stable in their ground state. Its binding energies are much smaller than Ge_{n+1}. $AsGe_{18}$ has a lowest-energy structure with C_1 point group symmetry. The As atom tends to be stabilized on the surface. The most favorable isomer for $AsGe_{19}$ cluster shows prolate-like and cage-like structures with C_1 symmetry and a calculated binding energy of 3.029 eV/atom, which is close to that of tetramer Ge_{20} (3.046 eV/atom). For n = 20, the lowest-energy isomer combines a prolate-like structure with the cage-like one. The binding energy

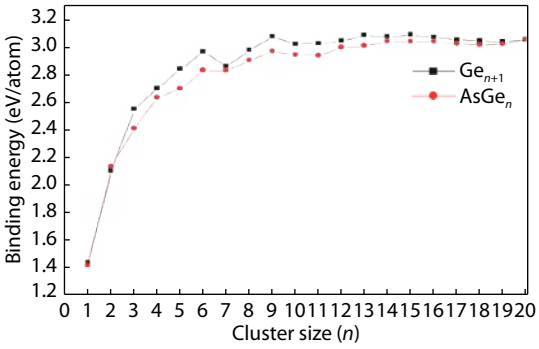

Fig. 3. (Color online) Evolution of the binding energy per atom for the lowest energy structures of Ge_{n+1} and $AsGe_n$ (n = 1–20) clusters as a function of cluster size.

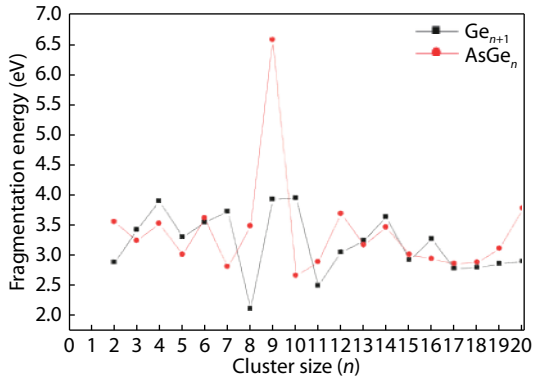

Fig. 4. (Color online) Evolution of the fragmentation energy of Ge_{n+1} and $AsGe_n$ (n = 1–20) clusters as a function of cluster size.

of $AsGe_{20}$ (0.004 eV/atom) is almost the same than that obtained for the ground state structure of the pure Ge_{21} cluster.

3.2. Relative stability

3.2.1. Binding energy

The size dependence on the binding energies per atom for the lowest energy structures of Ge_{n+1} and $AsGe_n$ (n = 1–20) clusters are shown in Fig. 3. As expected, the bonding energy gradually increases with increasing size, and this can be associated with the increasing average number of neighbors per atom. For $AsGe_n$, we observe that the binding energies are lower than those for Ge_{n+1}. This means that doping with As atoms has no immediate effects on enhancing the stability of germanium cluster at small size. In most of $AsGe_n$ clusters, the final structures do not differ from that of the corresponding pure germanium cluster. This may be due to the equivalence in the nature of bonding, the size and the atomic mass between the two metalloids arsenic and germanium used in this study. However, for n = 2 and n = 20 we observe that the binding energy per atom of $AsGe_n$ clusters is larger than those of corresponding pure Ge_{n+1} clusters. Then, the substituting a Ge atom by a As atom increases the stability these two clusters. An increase in the binding energy is obtained with 1.426 eV for n = 2 to 2.837 eV for n = 6, and then non-monotonic and slow growth could be reached until n = 20.

3.2.2. Fragmentation energy

Fig. 4 shows the plot of the size dependence on the fragmentation energies of Ge_{n+1} and $AsGe_n$ (n = 1–20) clusters. An oscillating behavior is observed. The clusters with large values of fragmentation energy are relatively stronger in thermodynamic stability than neighboring clusters. Consequently, the

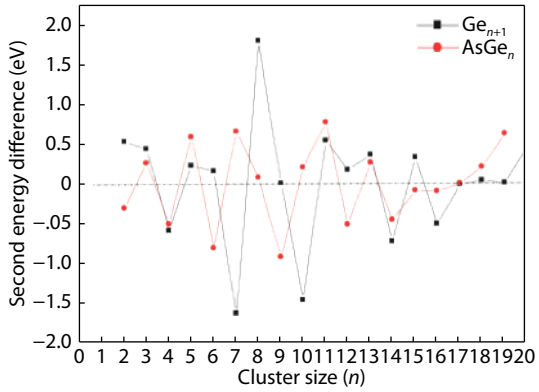

Fig. 5. (Color online) Evolution of the second-order difference of energy for the lowest energy structures of Ge_{n+1} and $AsGe_n$ (n = 1–20) clusters as a function of cluster size.

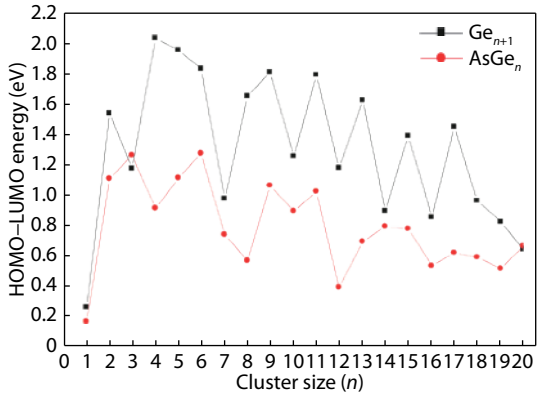

Fig. 6. (Color online) Evolution of the HOMO–LUMO gap for the lowest energy structures of Ge_{n+1} and $AsGe_n$ (n = 1–20) clusters as a function of cluster size.

thermodynamic stabilities of Ge_5, Ge_8, Ge_{10}, Ge_{11}, $AsGe_6$, $AsGe_9$, $AsGe_{12}$, and $AsGe_{20}$ clusters are relatively strong.

3.2.3. Second-order difference

The evolution of the second-order difference of energies for the most favorable structures of Ge_{n+1} and $AsGe_n$ (n = 1–20) clusters as a function of the cluster size is plotted in Fig. 5. The curve shows pronounced peaks for $AsGe_n$ at range size n = 3, 5, 7, 10, 11, 13, and 19 atoms. This suggests these clusters to be more favorable than their neighbors. . In cluster physics, if the values of Δ_2E are positive this means that the dissociation of As atom is an unfavorable process and the clusters are particularly stable. It can also be seen that the curve of Ge_{n+1} clusters with range size n = 2, 3, 5, 6, 8, 11, 12, 13, 15, and 20 exhibit higher stability than their neighbors. As a consequence, the stability of $AsGe_n$ structures with n = 3, 5, 11, 13 atoms correlates with the stability of the corresponding Ge_{n+1} structures, where the $AsGe_n$ structure was maintained the same upon the incorporation of As dopant.

3.3. Electronic properties

3.3.1. HOMO–LUMO gap

In order to obtain insight into the kinetic stability of $AsGe_n$ clusters, we calculated and analyzed the HOMO–LUMO gap. In general, the reactivity of the cluster decreases with increasing the HOMO–LUMO gap[28]. Fig. 6 reports the size dependence of HOMO–LUMO gap for the most favorable structures of Ge_{n+1} and $AsGe_n$ (n = 1–20) clusters. The decreasing behavior with

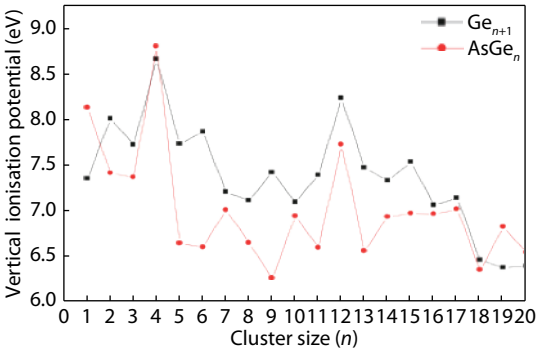

Fig. 7. (Color online) Evolution of the vertical ionization potential (VIP) for the lowest energy structures of Ge_{n+1} and $AsGe_n$ (n = 1–20) clusters as a function of cluster size.

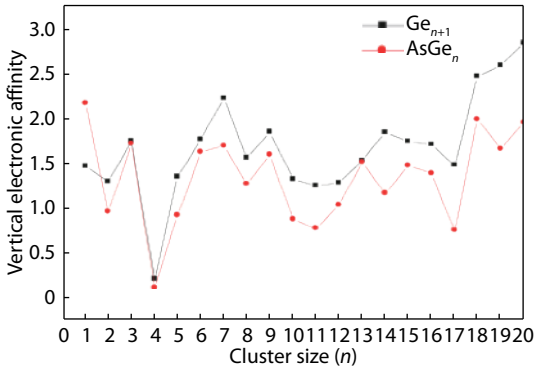

Fig. 8. (Color online) Evolution of the vertical electron affinity (VEA) for the lowest energy structures of Ge_{n+1} and $AsGe_n$ (n = 1–20) clusters as a function of cluster size.

the size is important for Ge_{n+1} clusters, while is less pronounced for $AsGe_n$ clusters. Overall, the gaps of $AsGe_n$ are much lower than those obtained for Ge_{n+1} clusters, except for n = 3 and 20, The value for $AsGe_n$ roughly oscillates in between 0.171 and 1.278 eV, which indicates a chemical activity increase of Ge_{n+1} clusters when doped with As. Doping Ge_{n+1} cages with an As atom leads to a significant HOMO–LUMO gap reduction in $AsGe_n$ clusters. This means that the chemical activity of $AsGe_n$ is higher than that of Ge_{n+1} clusters and the inserted As atom highlights the metallic character of $AsGe_n$ clusters. It should also be noted that Ge_4 cluster possesses the largest HOMO–LUMO gap of 2.036 eV, which indicates that Ge_4 cluster is expected to have an enhanced chemical stability. As a consequence, the substitution of an As atom would affect the chemical features of pure Ge_{n+1} clusters.

3.3.2. Vertical ionization potential (VIP) and vertical electronic affinity (VEA)

The size dependence on the vertical ionization potential (VIP) for the most favorable geometries of Ge_{n+1} and $AsGe_n$ (n = 1–20) clusters are displayed in Fig. 7. For $AsGe_n$ clusters, the VIP reveals an oscillating trend up to n = 14. All values are in the 6.2–8.8 eV range and decreases slowly as the cluster size increases and it is well known that when the VIP becomes smaller, the cluster will be more close to a metallic system. This means that the clusters of $AsGe_n$ with size more than 6 atoms exhibit high metallic character which, consequently, these clusters can more easily lose one electron comparatively to the clusters of smaller size. The smallest VIP values are observed for $AsGe_5$, $AsGe_6$, $AsGe_8$, $AsGe_9$, $AsGe_{11}$, $AsGe_{13}$, $AsGe_{18}$ and $AsGe_{20}$ indicating that these clusters are more readily ionized than the others. The cluster $AsGe_4$ has large VIP value (8.809). In Fig. 8, we plotted the cluster size-dependent VEA for Ge_{n+1} and $AsGe_n$ clusters. It can be seen that the electron affinity reveal also an oscillating trend with an increasing behavior with the size, which means the larger clusters are expected to capture more easily electrons more easily. This means that the small $AsGe_n$ clusters will become gradually unstable after they acquired an electron. The calculated values of VEA for the most stable $AsGe_n$ clusters are much lower than the VIP values which indicating that these clusters can easily accept one electron.

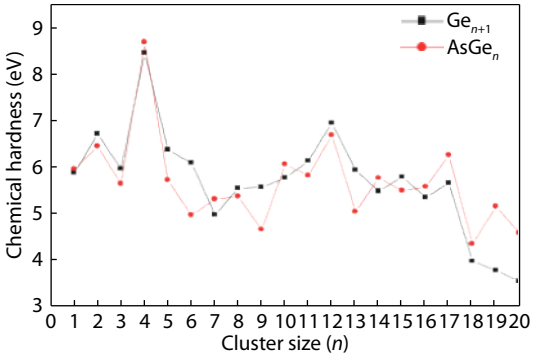

Fig. 9. (Color online) Evolution of the chemical hardness η for the lowest energy structures of Ge_{n+1} and $AsGe_n$ (n = 1–20) clusters as a function of cluster size.

3.3.3. Chemical hardness

Fig. 9 shows the evolution of the chemical hardness for the lowest energy structures of Ge_{n+1} and $AsGe_n$ (n = 1–20) clusters as a function of cluster size. Our calculations reveal that $AsGe_4$ clusters have the largest chemical hardness of 8.454 eV, confirming the better stability of this cluster as compared to the neighboring ones. Other local peaks are also observed for n = 12 and 17, leading to the conclusion that $AsGe_{12}$ and $AsGe_{17}$ will be less reactive than other cluster sizes. These clusters are very inert and can be considered as good candidates to the fabrication assembled cluster materials for application in nano-electronics and nanotechnologies. It has been established that chemical hardness is an electronic parameter that may characterize the relative stability of small clusters through the principle of maximum hardness (PMH) proposed by Pearson[39, 41]. The clusters with high values of hardness are less reactive and more stable.

4. Conclusion

We have systematically investigated the structural, energetic and electronic properties of Ge_{n+1} and $AsGe_n$ (n = 1–20) clusters by means of DFT-based first principles quantum computations. The $AsGe_n$ clusters adopted somehow similar structures as those obtained for Ge_{n+1} except for n = 8, 10, 11, and 16, which significantly differed from their corresponding Ge_{n+1}. In all cases, the As-doping atom was found to always be located on the surface. Their relative stabilities have been examined through the calculated binding energies, fragmentation energies, and second-order difference of energies. Their electronic features such as HOMO–LUMO energy gaps, vertical ionization potentials, vertical electron affinities, and chemical hardness were also examined.

Our theoretical study could give detailed and relevant information to deeply understand the possible effects of doping one single As atom on the properties of Ge_{n+1} clusters. We

believe this work will provide guidelines for future experimental work.

Acknowledgments

The authors thank Professor Ari Paavo Seitsonen (Ecole Normale Supérieure, ENS, Department of Chemistry, Paris, France) and Professor Bahayou Mohamed El Amine (Applied Mathematics Laboratory, LMA, Ouargla, Algeria) for all their advice and guidance.

References

[1] Wang J, Han J G. The growth behaviors of the Zn-doped different sized germanium clusters: a density functional investigation. Chem Phys, 2007, 342, 253

[2] Mahtout S, Tariket Y. Electronic and magnetic properties of Cr-Ge_n ($15 \leqslant n \leqslant 29$) clusters: a DFT study. Chem Phys, 2016, 472, 270

[3] Schmude R W, Gingerich K A. Thermodynamic study of small silicon carbide clusters with a mass spectrometer. J Phys Chem A, 1997, 101, 2610

[4] Samanta P N, Das K K. Electronic structure, bonding, and properties of Sn_mGe_n ($m + n \leqslant 5$) clusters: a DFT study. Comput Theor Chem, 2012, 980, 123

[5] Kingcade J Jr, Gingerich K. Knudsen effusion mass spectrometric investigation of palladium-germanium clusters. Inorg Chem, 1989, 28, 89

[6] Yadav P S, Yadav R K. Ab initio study of the physical properties of binary Si_mC_n ($m + n \leqslant 5$) nanoclusters. J Phys Cond Matter, 2006, 18, 7085

[7] Bandyopadhyay D, Kumar M. The electronic structures and properties of transition metal-doped silicon nanoclusters: a density functional investigation. Chem Phys, 2008, 353, 170

[8] Han J G, Hagelberg F. Recent progress in the computational study of silicon and germanium clusters with transition metal impurities. J Comput Theor Nanosci, 2009, 6, 257

[9] Bals S, Van Aert S, Romero C P, et al. Atomic scale dynamics of ultrasmall germanium clusters. Nat Commun, 2012, 3, 897

[10] Siouani C, Mahtout S, Safer S, et al. Structure, stability, and electronic and magnetic properties of VGe_n ($n = 1$–19) clusters. J Phys Chem A, 2017, 121, 3540

[11] Brack M. The physics of simple metal clusters: self-consistent jellium model and semiclassical approaches. Rev Mod Phys, 1993, 65, 677

[12] Han J G, Zhang P F, Lic Q X, et al. A theoretical investigation of Ge_nSn ($n = 1$–4) clusters. J Mol Struct, 2003, 624, 257

[13] Singh A K, Kumar V, Kawazoe, Y. Thorium encapsulated caged clusters of germanium: The Ge_n, $n = 16$, 18, and 20. J Phys Chem B, 2005, 109, 15187

[14] Wang J, Han J G. A computational investigation of copper-doped germanium and germanium clusters by the density-functional theory. J Chem Phys, 2005, 123, 244303

[15] Zhao W J, Wa ng, Y X. Geometries, stabilities, and magnetic properties of $MnGe_n$ ($n = 2$–16) clusters: density-functional theory investigations. J Mol Struct, 2009, 901, 18

[16] Jaiswal S, Kumar V. Growth behavior and electronic structure of neutral and anion $ZrGe_n$ ($n = 1$–21) clusters. Comput Theor Chem, 2016, 1075, 87

[17] Mahtout S, Siouani C, Rabilloud F. Growth behavior and electronic structure of noble metal-doped germanium clusters. J Phys Chem A, 2018, 122, 662

[18] Djaadi S, Aiadi K E, Mahtout S. First principles study of structural, electronic and magnetic properties of $SnGe_n$ ($0, \pm 1$)($n = 1$–17) clusters. J Semicond, 2018, 39, 042001

[19] Ordejón P, Artacho E, Soler J M. Self-consistent order-N density-functional calculations for very large systems. Phys Rev B, 1996, 53, R10441

[20] Soler J M, Artacho E, Gale J D, et al. The siesta method for ab initio order-n materials simulation. J Phys Cond Matter, 2002, 14, 2745

[21] Troullier N, Martins J L. Efficient pseudopotentials for plane-wave calculations. Phys Rev B, 1991, 43, 1993

[22] Perdew J P, Zunger A. Self-interaction correction to density-functional approximations for many-electron systems. Phys Rev B, 1981, 23, 5048

[23] Perdew J P, Burke K, Ernzerhof M. Generalized gradient approximation made simple. Phys Rev Lett, 1996, 77, 3865

[24] Bandyopadhyay D, Sen P. Density functional investigation of structure and stability of Ge_n and Ge_nNi ($n = 1$–20) clusters: validity of the electron counting Rule. J Phys Chem A, 2010, 114, 1835

[25] Shi S, Liu Y, Zhang C, et al. A computational investigation of aluminum-doped germanium clusters by density functional theory study. Comput Theor Chem, 2015, 1054, 8

[26] Kapila N, Garg I, Jindal V K, et al. First principle investigation into structural growth and magnetic properties in Ge_nCr clusters for $n = 1$–13. J Mag Mag Mater, 2012, 324, 2885

[27] Wang J, Wang G, Zhao J. Structure and electronic properties of Ge_n ($n = 2$–25) clusters from density-functional theory. Phys Rev B, 2001, 64, 205411

[28] Yoshida M, Aihara J I. Validity of the weighted HOMO–LUMO energy separation as an index of kinetic stability for fullerenes with up to 120 carbon atoms. Phys Chem Chem Phys, 1999, 1, 227

[29] Parr R G, Pearson R G. Absolute hardness: companion parameter to absolute electronegativity. J Am Chem Soc, 1983, 105, 7512

[30] Sosa-Hernández E, Alvarado-Leyva P. Magnetic properties of stable structures of small binary Fe_nGe_m ($n + m \leqslant 4$) clusters. Physica E, 2009, 42, 17

[31] Li X, Su K, Yang X, et al. Size-selective effects in the geometry and electronic property of bimetallic Au-Ge nanoclusters. Comput Theor Chem, 2013, 1010, 32

[32] Kingcade J E, Nagarathna-Naik H M, Shim I, et al. Electronic structure and bonding of the dimeric germanium molecule from all-electron ab initio calculations and equilibrium measurements. J Phys Chem, 1986, 90, 2830

[33] Nagendran S, Sen S S, Roesky H W, et al. RGe(I)Ge(I)R Compound ($R = PhC(NtBu)_2$) with a Ge–Ge single bond and a comparison with the gauche conformation of hydrazine. Organometallics, 2008, 27, 5459

[34] Gadiyak G V, Morokov Y. N, Mukhachev A G, et al Electron density functional method for molecular system calculations. J Struct Chem, 1982, 22, 670

[35] Wang J, Han J G. Geometries, stabilities, and vibrational properties of bimetallic Mo_2-doped Ge_n ($n = 9$–15) clusters: a density functional investigation. J Phys Chem A, 2008, 112, 3224

[36] Kant A, Strauss B H. Atomization energies of the polymers of germanium, Ge_2 to Ge_7. J Chem Phys, 1966, 45, 822

[37] Vasiliev I S, Öğüt S, Chelikowsky J R. Ab initio calculations for the polarizabilities of small semiconductor clusters. Phys Rev Lett, 1997, 78, 4805

[38] Burton G R, Xu C, Arnold C C, et al. Photoelectron spectroscopy and zero electron kinetic energy spectroscopy of germanium cluster anions. J Chem Phys, 1996, 104, 2757

[39] Safer S, Mahtout S, Rezouali K, et al. Properties of neutral and charged cobalt-doped arsenic $CoAs_n$ (0 ± 1) ($n = 1$–15) clusters by density functional theory. Comput Theor Chem, 2016, 1090, 23

[40] Guo L. The structure and energetic of $AlAs_n$ ($n = 1$–15) clusters: a first-principles study. J Alloys Compounds, 2010, 498, 121

[41] Pearson R G. Chemical hardness: applications from molecules to solids. Weinheim: Wiley-VCH, 1997